A strain-tunable nanoimprint lithography for linear variable photonic crystal filters

Longju Liu[1], Haris A Khan[2], Jingjing Li[2], Andrew C Hillier[3] and Meng Lu[1,4]

[1] Department of Electrical and Computer Engineering, Iowa State University, Ames, IA 50011, USA
[2] Department of Mechanical Engineering, University of Hawaii, Honolulu, HI 96822, USA
[3] Department of Chemical and Biological Engineering, Iowa State University, Ames, IA 50011, USA
[4] Department of Mechanical Engineering, Iowa State University, Ames, IA 50011, USA

E-mail: menglu@iastate.edu

CrossMark

Abstract

This paper presents the fabrication methodology of a linear variable photonic crystal (PC) filter with narrowband reflection that varies over a broad spectral range along the length of the filter. The key component of the linear variable PC filter is a polymer surface-relief grating whose period changes linearly as a function of its position on the filter. The grating is fabricated using a nanoreplica molding process with a wedge-shaped elastomer mold. The top surface of the mold carries the grating pattern and the wedge is formed by a shallow angle between the top and bottom surfaces of the mold. During the replica molding process, a uniaxial force is applied to stretch the mold, resulting in a nearly linearly varying grating period. The period of the grating is determined using the magnitude of the force and the local thickness of the mold. The grating period of the fabricated device spans a range of 421.8–463.3 nm over a distance of 20 mm. A high refractive index dielectric film is deposited on the graded-period grating to act as the waveguide layer of the PC device. The resonance reflection feature of the device varies linearly in a range of 680.2–737.0 nm over the length of the grating.

S Online supplementary data available from stacks.iop.org/NANO/27/295301/mmedia

Keywords: linear variable filters, photonic crystals, nanoimprint lithography, strain

(Some figures may appear in colour only in the online journal)

Introduction

Variable optical filters are designed to exhibit graded transmittance or reflectance depending on the location, where the measurement is performed on the filter [1–3]. Among the many types of variable filters, the linear variable bandpass filter, with a peak transmission wavelength varying linearly in one direction and remaining uniform in the other direction, is most popular. This type of optical filter is desirable for several applications, including in a compact spectrum analyzer, where the filter is directly attached to a charge-coupled device sensor, and for use as a color filter in hyperspectral imaging [4, 5]. The linear variable effect can be achieved by using a Fabry–Perot cavity with a linearly graded cavity length. While Fabry–Perot interference filters are used for such purposes, other methods may offer a lower cost, a narrower bandwidth, and an improved wavelength range. One-dimensional photonic crystals (PC), with a grating-coupled waveguide, which support guided-mode resonance (GMR), have demonstrated the extraordinary ability of generating narrowband reflections at specific wavelengths [6–8]. Dobbs *et al* [9] reported a PC-based linear variable filter that uses a grating structure in conjunction with a waveguide layer whose thickness progressively changes. PC-based devices have also been found to be useful for a variety of other applications, including spectrum analysis, optical biosensors, optical communications, and displays [10–12]. The optical characteristics of a PC filter, such as the resonance wavelength, peak reflection efficiency, and linewidth, can be engineered by controlling the geometrical parameters of the device and its component materials [13, 14]. Currently, the application of the PC devices is mainly challenged by the demanding fabrication processes required to produce gratings on a sub-micrometer scale.
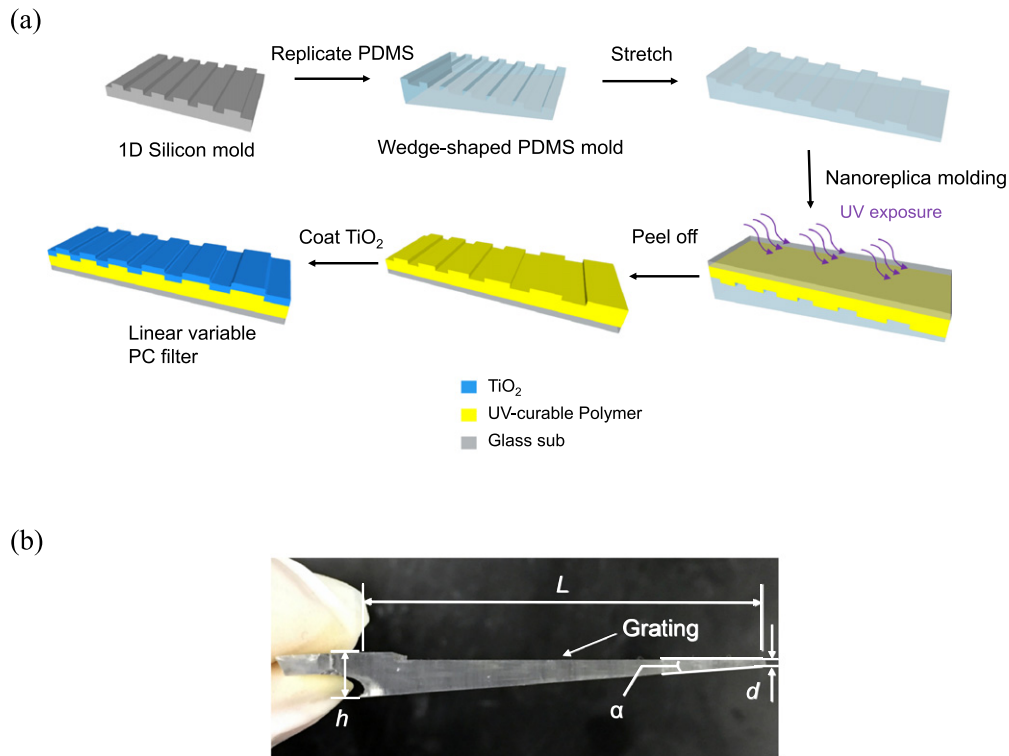
Figure 1. (a) Schematic of the linear variable replica molding process. (b) A photo showing the dimensions of the replicated wedge-shaped PDMS.

Conventional lithography methods, such as electron beam lithography and deep UV lithography, are expensive with limited throughput. Recently, techniques, such as interference lithography and soft lithography, have been successfully applied for the fabrication of PC devices [15, 16]. In particular, nanoreplica molding, as a soft lithography process, allows inexpensive fabrication of nanoscale gratings by transferring the pattern of a mold to a target substrate using photocurable or thermally curable polymer materials [17, 18].

In this work, we present a PC filter that exhibits a spatially variable resonant reflection along the length of the filter. The device is fabricated using nanoreplica molding with a wedge-shaped polydimethylsiloxane (PDMS) mold. During the nanoreplica molding process, the elastic PDMS mold is deliberately stretched to generate surface-relief gratings with a linearly graded period along the length of the device. When the elastic mold is elongated by 22.3%, the grating period spans a range of approximately 421.8–463.3 nm across the 20 mm length. Following replica molding, the gratings are coated with a 160 nm thick titanium dioxide (TiO_2) dielectric film, which functions as the light-confinement layer of the PC filter. The PC filter is then characterized via optical reflection to show the graded resonant reflection in the wavelength range of 680.2–737.0 nm with a gradient of 2.85 nm mm^{-1}.

Methodology

The proposed replica molding process for the fabrication of linear variable PC filters is summarized in figure 1(a).

The key steps of the process include mold preparation, mold stretching, pattern transfer, and mold release. The first step is the preparation of the PDMS mold of the desired grating pattern, with a negative surface profile and linearly increasing thickness. The PDMS mold used to fabricate the PC device was cast from a silicon master wafer bearing a uniform grating pattern with a period, depth, and duty cycle of 360 nm, 60 nm, and 40%, respectively. The grating on the silicon master wafer was fabricated using deep UV photolithography and reactive ion etching. To obtain the PDMS mold, the silicon master wafer was placed in a petri dish with 15 g of uncured PDMS (Sylgard 184). In order to ensure the PDMS mold was tapered, a 30 mm thick acrylic block, which was tilted at an angle to the top surface of the silicon master wafer, was used to form the uncured PDMS into a wedge shape as shown in figure S1[5]. The inclination angle α was carefully controlled to generate the desired wedge shape for the PDMS mold. The PDMS wedge was thermally cured (70 °C, 4 h) and then slowly separated from the silicon master and the acrylic bar. Figure 1(b) shows the fabricated PDMS wedge with an inclination angle, base height, rise, and length of $\alpha = 4.8°$, $h = 4.1$ mm, $d = 1$ mm, and $L = 36.7$ mm, respectively. The tapered ends of the PDMS mold were aligned parallel to the grating (figure 1(a)). Subsequently, the elastic PDMS mold was stretched to produce a surface with a linearly graded period. As shown in figure 1(a), a uniaxial force was applied

---

[5] See supplemental material at stacks.iop.org/NANO/27/295301/mmedia for the fabrication method of wedge-shaped PDMS mold, the SEM images and the AFM images of the linear variable PC filter.
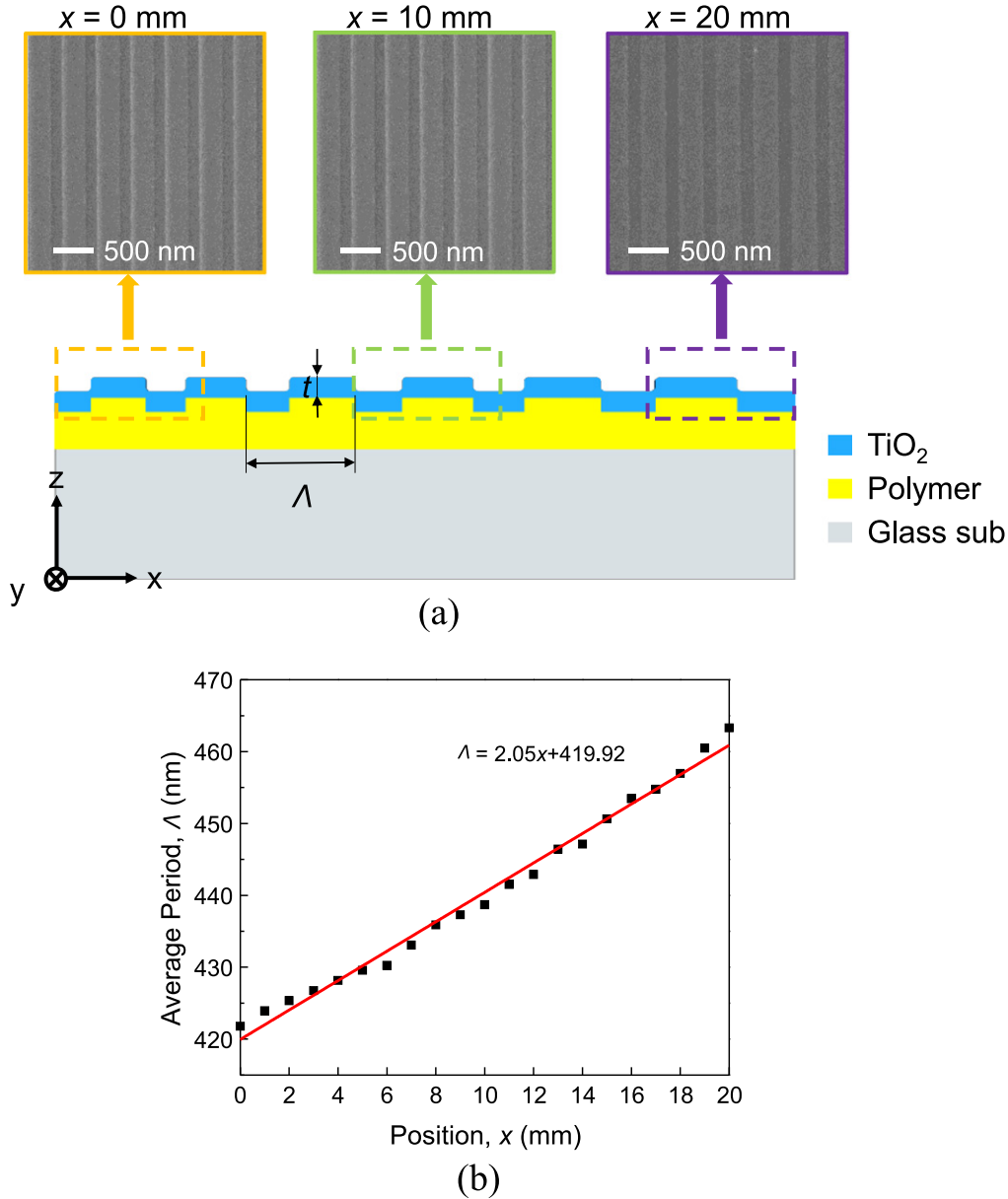
Figure 2. (a) Schematic cross section of the PC filter structure (not to scale) and the SEM images of the replicated grating at three different positions on the sample. The labeled x values represent the locations of the measurements along the gradient direction of the PC filter sample. The grating periods of the left panel, center panel, and right panels are $\Lambda = 421.8$ nm, $\Lambda = 438.7$ nm, and $\Lambda = 463.3$ nm, respectively. (b) Measured grating periods as a function of lateral position on the fabricated PC filter. The periods were at positions between $x = 0$ mm and $x = 20$ mm with increment of 1 mm. The coefficient of determination, R^2 for the linear fitting (red line) is 0.989.

to the PDMS mold perpendicular to the grating direction. As a result, the one-dimensional grating structure was stretched and its period increased depending on its position along the PDMS wedge. The local strain can be represented by $\varepsilon(x) = \frac{F}{w t(x) E_{PDMS}}$, where F is the applied force, E_{PDMS} is the Young's Modulus of the cured PDMS, x is the position on the mold along the stretched direction, and w and $t(x)$ are the width and the thickness of the mold, respectively. As shown in figure 1(b), the thickness of the mold can represented with the linear expression $t(x) = h + (L - x)\tan(\alpha)$. The local strain $\varepsilon(x)$ is large where the PDMS mold is thin, and vice versa. Consequently, the elongation of the grating is a function of the position along the PDMS mold,

$\Delta\Lambda(x) = \Lambda_0 \varepsilon(x) = \Lambda_0 \frac{F}{w\{h + (L - x)\tan(\alpha)\} E_{PDMS}}$, where Λ_0 is the unstretched grating period. The grating pattern on the stretched PDMS mold was replicated onto a glass substrate using the nanoreplica molding process. Briefly, a layer of liquid UV-curable polymer (Norland Optical Adhesive 88) was squeezed between the stretched PDMS mold and a glass substrate. The liquid polymer was then cured by exposing to UV light (Spectroline Spectrolinker XL-1500) with a dose of 120 mJ cm^{-2}. Once exposed to UV light, the UV-curable polymer was solidified and subsequently released from the PDMS mold. Because the PDMS surface is hydrophobic without any special surface treatment, the cured polymer layer preferentially sticks to the glass substrate. Following replica

molding, a dielectric thin film was deposited over the replicated polymer grating as the waveguide layer for the PC structure. In this example, a 160 nm thick film of TiO$_2$ (refractive index = 2.1) was deposited using an electron beam evaporator.

A schematic cross-sectional diagram of the linear variable PC device is shown in figure 2(a). On a macroscopic scale, the grating period Λ is non-uniform and dependent on its location along the length of the PC filter. In this work, the PC device was fabricated when the PDMS mold was stretched to 122.3% of its original length. Scanning electron microscopy (SEM) images in figure 2(a) were taken at three locations along the sample, corresponding to the far left ($x = 0$ mm), center ($x = 10$ mm), and the far right spot ($x = 20$ mm). Using the SEM images, the period was calculated as an average across eight ridge/groove pairs with ImageJ. The measured value of the periods from the SEM images was $\Lambda = 421.8$ nm ($x = 0$ mm), $\Lambda = 438.7$ nm ($x = 10$ mm), and $\Lambda = 463.3$ nm ($x = 20$ mm). To further investigate the relationship between the grating period and the position, the grating period was measured using the SEM images (figure S2 in the supplemental material) at 20 different locations ranging from $x = 0$ to $x = 20$ mm with an increment of 1 mm. The measured grating periods as a function of lengthwise location are summarized in figure 2(b). In an effort to study the linearity of the relationship, the data was fitted with a linear function, as illustrated in figure 2(b). The coefficient of determination is $R^2 = 0.989$ for the fit, suggesting a nearly linear dependency of the period on the location along the length of the PC device. We also confirmed the morphology of the fabricated device using an atomic force microscope (AFM). The AFM images in figure S3 (see footnote 5) show the grating depth decreases from 60 to about 25 nm due to the stretch-induced compression along the surface normal of the grating. Later on, the change of grating depth can be taken into account during the design of the grating pattern of the silicon master wafer.

Results and discussions

For identifying the optical resonances of the graded PC filter, numerical simulations of the replicated polymer grating coated with a 160 nm thick TiO$_2$ film were performed. The periodic PC structure was modeled using rigorous coupled wave analysis (RCWA). Since the PC structure is polarization dependent, the numerical model used a linearly polarized incident light with the electric field parallel to the grating lines to excite the transverse electric (TE) modes. The incident beam was normal to the PC surface. The refractive indices of the polymer grating and TiO$_2$ film were 1.47 and 2.2, respectively. The grating depth was 25 nm. The grating periods used in the RCWA simulation were obtained from the measurement results shown in figure 2(b). Figure 3 shows the calculated transmission spectra at 11 different positions spanning a distance of 20 mm along the sample with increments of 2 mm. As expected, the wavelength of the transmission dip increases with increasing grating period. The resonance wavelength, which is
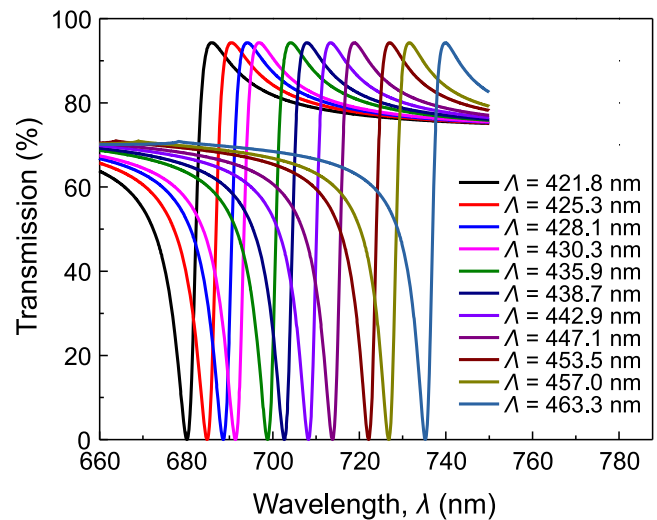
Figure 3. Calculated transmission spectra obtained by the RCWA simulation for the graded PC filter at 11 locations spanning 20 mm with increments of 2 mm.

referred to as the wavelength at the minimal transmittance, varies from 680.3 to 735.3 nm with a full-width half-maximum (FWHM) of approximately 7 nm.

To experimentally characterize the optical resonances of the graded PC filter, transmission spectra of the fabricated device were measured at the positions mentioned in the above numerical study. The measurement setup used a halogen lamp as the excitation source, which was coupled to a multimode fiber with a fiber tip collimator. An iris and a linear polarizer were placed in front of the collimator to control the spot size and polarization of the incident beam, respectively. The transmitted light was collected by another fiber and recorded by a spectrometer (USB2000, OceanOptics). The PC device was mounted on a motorized stage that translated the device along the gradient direction of the grating period. The orientation of the device was adjusted to the normal-incidence condition. Figure 4(a) shows the measured transmission spectra with TE polarization at 11 locations from $x = 0$ to $x = 20$ mm. At $x = 0$ mm, the resonance wavelength is 680 nm, and the resonance gradually shifts to 737 nm at $x = 20$ mm. This result clearly demonstrates that the spectral position of the optical resonance is directly related to the location of measurement for the PC device.

Figure 4(b) shows the dependence of resonance wavelength on the lateral position along the gradient direction of the grating period. The measured spectra are each fitted using a second-order polynomial function to determine the resonance wavelengths. For comparison, the result of the numerical simulation is plotted in red. The total shift of the resonance wavelength is 57 nm over a distance of 20 mm, resulting in a gradient of 2.85 nm mm^{-1}. The data points were fitted with a linear curve to demonstrate the dependence of the resonance wavelength on the location of measurement for the PC filter. According to the coefficients of determination, the relationship is quite linear, owing to the nearly linear change of the grating period and the linear relationship between grating period and resonance wavelength within the
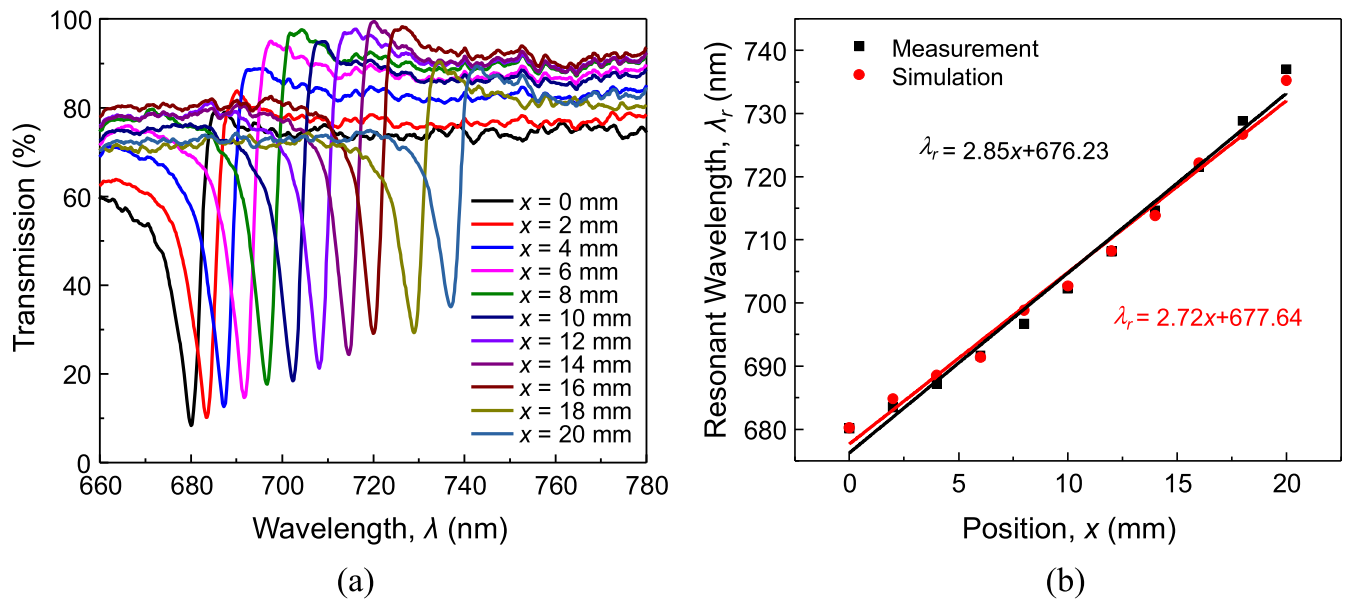
Figure 4. (a) Measured transmission spectra with TE polarization at the 11 locations specified in the numerical study. (b) Dependence of measured and calculated resonant wavelengths on the lateral position. The resonant wavelengths are fitted by the solid lines, which show a high degree of linearity with coefficient of determination, R^2 of 0.983 and 0.986, respectively.
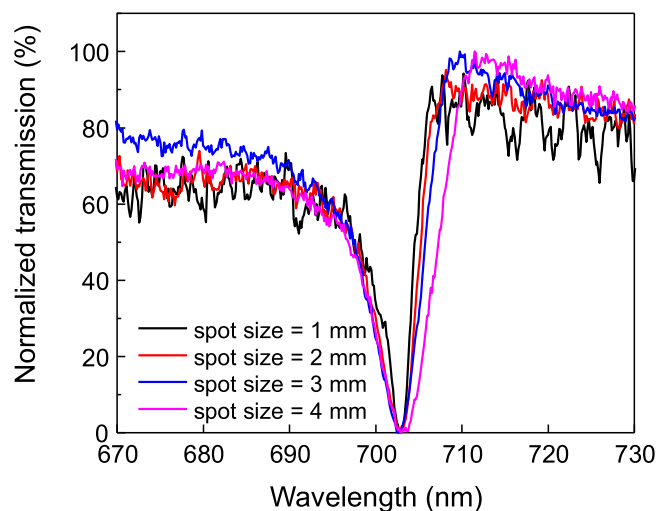
Figure 5. Measured transmission resonance at $x = 10$ mm with spot sizes 1, 2, 3, and 4 mm. The FWHM of the resonances are 6.5 nm, 7.8 nm, 8.4 nm, and 10.4 nm, respectively.

wavelength range of this study. In addition, figures 3 and 4 show good agreement between the simulation and experimental results.

The spectral bandwidth is one of the performance metrics of linear variable filters. There are two factors that determine the bandwidth of a graded PC structure. The first factor is the linewidth of the guide-mode resonance, and the second is the spatial gradient of the resonance. We studied the dependence of the bandwidth on the spot size of the light beam in order to clarify the effect of each factor. An iris was placed in front of the PC device to control the beam spot size. Figure 5 shows the normalized transmission spectra measured at the center of the filter ($x = 10$ mm) with spot sizes of 1, 2, 3, and 4 mm. When the beam spot size decreases from 4 to 2 mm, the

FWHM reduces from 10.4 to 7.8 nm. Future reduction of the spot size from 2 to 1 mm reduces the FWHM from 7.8 to only 6.5 nm. With a beam spot size of 1 mm, the measured bandwidth is close to that of the RCWA simulation, which ignores the variation of the grating period. Therefore, when the beam size is as small as 1 mm, the bandwidth is limited by the resonance linewidth, rather than the gradient effect. The bandwidth of the fabricated variable filter is comparable to the commercial products. For example, the FWHM of the linear variable VIS to NIR bandpass filter (LVVISNIRBP, Delta Optical Thin Film) is approximately 10 nm in the same wavelength range.

Conclusions

In summary, a new approach was developed to fabricate a PC device with a linear variable resonance along its length. The fabrication approach is based on the nanoreplica molding process and uses a stretchable PDMS wedge as the mold. During the molding process, stress is applied to the PDMS mold, generating elongations as a function of the specific location on the wedge-shaped mold. The elongation of the grating on the mold surface is determined by the local thickness of the mold, the applied stress, and the Young's modulus of the PDMS. The period of the replicated polymer grating spans a range of 421.8–463.3 nm over a distance of 20 mm. The results of the optical characterization show that the resonance wavelength of the PC filter varies across a spectral range of 57 nm with a gradient of 2.85 nm mm^{-1}. The linear variable PC device has a number of potential applications. In particular, the narrow bandwidth feature of the GMR mode is desirable for spectral analysis and can be utilized to build a miniaturized spectrometer [19]. The

performance of the PC filter will be further improved by implementing the three-layer PC structure to obtain a transmission resonance and a reduced linewidth of the resonance [20].

Acknowledgments

References

[1] Emadi A, Wu H, Grabarnik S, De Graaf G, Hedsten K, Enoksson P, Correia J H and Wolffenbuttel R F 2010 *Sensors Actuators* A **162** 400

[2] Piegari A and Bulir J 2006 *Appl. Opt.* **45** 3768

[3] Piegari A, Bulir J and Sytchkova A K 2008 *Appl. Opt.* **47** C151

[4] Kiesel P, Schmidt O, Mohta S, Johnson N and Malzer S 2006 *Appl. Phys. Lett.* **89** 201113

[5] Emadi A, Wu H W, de Graaf G and Wolffenbuttel R 2012 *Opt. Express* **20** 489

[6] Wang S S, Magnusson R, Bagby J S and Moharam M G 1990 *J. Opt. Soc. Am.* A **7** 1470

[7] Ding Y and Magnusson R 2004 *Opt. Express* **12** 1885

[8] Rosenblatt D, Sharon A and Friesem A A 1997 *IEEE J. Quantum Electron.* **33** 2038

[9] Dobbs D W, Gershkovich I and Cunningham B T 2006 *Appl. Phys. Lett.* **89** 123113

[10] Magnusson R and Shokooh-Saremi M 2007 *Opt. Express* **15** 10903

[11] Uddin M J and Magnusson R 2012 *IEEE Photonics Technol. Lett.* **24** 1552

[12] Block I D, Ganesh N, Lu M and Cunningham B T 2008 *IEEE Sensors J.* **8** 274

[13] Day R W, Wang S S and Magnusson R 1996 *J. Lightwave Technol.* **14** 1815

[14] Liu J N, Schulmerich M V, Bhargava R and Cunningham B T 2014 *Opt. Express* **22** 18142

[15] Xia Y N and Whitesides G M 1998 *Angew. Chem., Int. Ed. Engl.* **37** 551

[16] Lu C and Lipson R H 2010 *Laser Photonics Rev.* **4** 568

[17] Ahn S H and Guo L J 2009 *ACS Nano* **3** 2304

[18] Liu L, Zhang J, Badshah M A, Dong L, Li J, Kim S-M and Lu M 2016 *Sci. Rep.* **6** 22445

[19] Ganesh N, Xiang A, Beltran N B, Dobbs D W and Cunningham B T 2007 *Appl. Phys. Lett.* **90** 081103

[20] Niraula M, Yoon J W and Magnusson R 2014 *Opt. Express* **22** 25817